

Advanced photochemical processes for the manufacture of nanopowders: an evaluation of long-term pilot plant operation

Supplementary Information

Jan Bárta^[a], Lenka Prouzová Procházková^[a,b], Michaela Škodová^[a], Kateřina Děcká^[a], Kseniya Popovich^[a], Tereza Janoušková Pavelková^[a], Patrik Beck^[c] and Václav Čuba^[a,*]

a Department of Nuclear Chemistry, Faculty of Nuclear Sciences and Physical Engineering, Czech Technical University in Prague, Břehová 7, 115 19 Prague 1, Czech Republic

b Institute of Physics, Czech Academy of Sciences, Cukrovarnická 10, 162 00 Prague 6, Czech Republic

c Tesla V.T. Mikroel, Nademlejnská 600/1, 198 00 Prague 9, Czech Republic

* corresponding author: vaclav.cuba@fffi.cvut.cz

Cost calculations for production of nanomaterials using the photochemical pilot plant

The following chapters summarize the assumptions and approaches used for the calculation of production costs of nanomaterials investigated in this work.

1) Process parameters used in the calculations

Experimental parameters of a broad selection of syntheses performed in the discussed photochemical pilot plant are summarized in Table SII. In some cases, the product was not separated using the typical procedure (i.e. decantation and microfiltration), so there are some additional product losses in those experiments and the synthesis yield is thus lower compared to chemical yield. Additionally, the synthesized gelatinous material was centrifuged in one experiment (1 mM YAG) and used directly as a thick gel, with only an approximate estimation of synthesis yield.

To ensure better comparability of all associated costs, the costs were always normalized to the total synthesis yield achieved within the pilot plant (see Table SII). For garnets, the linear behaviour was exploited and the fit from Fig. 4 was used as the synthesis duration for a given concentration (i.e. 21.8 h for 2 mM garnet) with 93% yield. In the evaluation of remaining syntheses, the actual duration of irradiation in the pilot plant was utilized.

Additionally, the same values were calculated for a 100 % synthesis yield (for identical irradiation time) as well to

provide the theoretical minimum costs associated with the given part of the process. In the following chapters, both the experimental values, and the theoretical limits will be used to calculate respective costs.

Table SII – A selection of preparative experiments performed using the photochemical pilot plant and the amount of final product (heat treated to garnets or ZnO).

Material (solution composition)	Duration [h]	Product amount [g]	
		achieved	theoretical
GGAG, 2 mM	24.4*	130.2	139.7
YAG, 0.5 mM	5.75	~21	23.7
YAG, 2.5 mM	20.0 [†]	~95	118.7
YAG, 3 mM	30.7	132.0	142.5
YAG, 4 mM	44.0	180.1	190.0
YAG, 5 mM	40.0 [†]	203.3	237.4
ZnO – hydrozincite, Zn ₅ (OH) ₆ (CO ₃) ₂			
10 mM Zn ²⁺ , 0.2 M H ₂ O ₂	6.6	29.5	65.1
50 mM Zn ²⁺ , 0.5 M H ₂ O ₂	5.0	274	325.5
ZnO – zinc peroxide, ZnO ₂			
20 mM Zn ²⁺ , 1 M H ₂ O ₂	21.0	38.3	130.3
50 mM Zn ²⁺ , 1 M H ₂ O ₂	24.0	110.2	321.6

* possibly excessive irradiation, [†] insufficient irradiation time

2) Capital costs φ [€/g]

The initial investment into the photochemical pilot plant (purchase of the equipment) can be incorporated into the cost calculations through depreciation as capital costs φ . Thus, the 5-year depreciation period of the equipment and useable operational time of 49 weeks a year was assumed. For the pilot plant equipment, 104 hours a week was considered (overnight operation, 4×24 + 8 h), totalling depreciation over a **25 480 h period**. However, the UV lamps used have a lower rated average lifetime of 16 000 h; therefore, we assumed for the evaluation of capital costs that the lamps will be exchanged after 12 800 h (80 % of rated lifetime) of operation. The value of all equipment was based on the actual purchase price (VAT excluded) of the described pilot plant components (see Table SI2) or market prices and includes a 15 % surcharge for maintenance, if applicable.

The capital costs also have to include the hourly depreciation of the model furnace described in 4), which was estimated at 0.286 €/h of furnace time; this assumes an approximate purchase value of 8 400 € excl. VAT and operational time of 5×24 h a week (**29 400 h** in total).

The summary of capital costs for the production of all studied nanomaterials is provided in Table SI3 as € per g of the final material after heat treatment, i.e. nanocrystalline garnet or ZnO phase.

Table SI2 – Hourly depreciation of the photochemical pilot plant components (prices are VAT excluded).

Component	Price [€]	Depreciation [€/h]	Note
Glass reactor	6 000	0.235	*
Water chiller	2 430	0.095	
Stirrer	2 010	0.079	
Peristaltic pump	185	0.007	
Immersible UV lamp system	7 754	0.304	
Replacement lamps T5Q408-4P-44W	1 674	0.066	
Total	20 053	0.787	

* does not include maintenance surcharge

Table SI3 – The breakdown of capital costs φ for nanomaterial production in the pilot plant, including the required furnace time depreciation (see 4)) and their theoretical limits for 100 % yield.

Material (solution composition)	$\varphi_{\text{preparation}}$ [€/g*]		$\varphi_{\text{treatment}}$ [€/g*]
	exp.	limit	
2 mM YAG	0.194	0.181	0.0167 ¹
2 mM GGAG	0.130	0.121	0.0118 ¹
hydrozincite, Zn ₅ (OH) ₆ (CO ₃) ₂			
10 mM Zn ²⁺	0.177	0.080	0.0085 ²
50 mM Zn ²⁺	0.014	0.012	
zinc peroxide, ZnO ₂			
20 mM Zn ²⁺	0.432	0.127	0.0048 ³
50 mM Zn ²⁺	0.171	0.058	

* mass of final product (garnet or ZnO); ¹ 1200 °C / 2 h, 15 °C/min; ² 700 °C / 2 h, 15 °C/min; ³ 200 °C / 2 h, 2 °C/min

3) Raw materials costs χ [€/g]

The cost of raw materials strongly depends on their purity and the basis for the assay specifications (chemical identity or trace metals), under which they are marketed. In the described photochemical processes, neither chemical purity of the anions (e.g. presence of some acetate in ammonium formate or chloride in nitrates), nor presence of alkali metals affect the product or process significantly. The alkali metal compounds feature extreme solubility in aqueous solutions and cannot be expected in a formed solid phase in substantial amounts. However, trace (heavy) metal purity is much more important, as the luminescent properties of materials reflect low concentrations of dopants, even ppm values being readily observable in some cases. Therefore, for cost calculations, chemicals with ~ 4N trace metal purity (99.99 %) available at a single supplier were used (Alfa Aesar has been chosen arbitrarily, VAT excluded), for the highest available batch size. For raw materials without nominal metal ions or where the stated purity was based on chemical identity, the “per analysis” chemical grade was selected and the specification sheets were consulted to verify a low trace metal content below ~ 0.01% (excluding alkali metals). The materials considered for the

cost calculation are summarized in Table SI4; for simplicity, dissolution of all oxides in diluted nitric acid was assumed. Note that α -Al₂O₃ is virtually insoluble in common acids, so it cannot be used as a starting chemical, and though the commercial β -Ga₂O₃ has been dissolved in an excess of hydrochloric acid in this work, the substitution for nitric acid in cost calculations will not affect χ significantly.

Table SI4 – Raw materials used for the cost calculations, along with their purity and market price (excl. VAT) from Alfa Aesar, March 2021.

Chemical	Amount	Price [€]	Cost [€/g]
Ga ₂ O ₃ , 5N	100 g	817	8.170
Gd ₂ O ₃ , 4N	1 000 g	605	0.605
Y ₂ O ₃ , 4N	1 000 g	488	0.488
ZnO, 4N	250 g	96	0.384
Al(NO ₃) ₃ ·9H ₂ O, 98%*	5 000 g	276	0.055
HCOONH ₄ , 97%*	5 000 g	201	0.040
HNO ₃ , 68–70% ACS*	19 068 g	409	0.021
H ₂ O ₂ , 35%*	1000 mL	47	0.047†

* chemical identity-based purity; † in g/mL

Raw materials costs per obtained product mass necessarily include purified water (type II). To calculate it, we assumed a 3000 € reverse-osmosis system operated for 49 weeks a year, 5 days a week that generates 160 litres of purified water each working day. The annual maintenance costs (filters and ion-exchange resin exchange every 3 months) were assumed to be 320 €; along with a 5-year depreciation of the water purification system, this leads to an average water costs of 0.023 €/dm³ (1.878 € for a single synthesis using 80 dm³ of purified water). These assumptions were based on the performance of the water purification system used for the discussed photochemical pilot plant.

The calculated values of raw materials costs are summarized in Table SI5. The Gd₃Ga₂Al₃O₁₂ (GGAG) synthesis features markedly higher χ than Y₃Al₅O₁₂ (YAG), mainly because of the very costly Ga₂O₃; in both

cases, the theoretical limit is quite close to the experimental values due to very good yields. A much higher difference between the experimental χ and its limit value was calculated for ZnO₂ syntheses due to rather low synthesis yields. In spite of the relative cheapness of zinc compounds, even the theoretical limits for ZnO production through both precursors are quite high due to a substantial volumes of H₂O₂ used in the synthesis.

Table SI5 – The raw materials costs for synthesis of studied nanomaterials along with their theoretical limits for 100 % yield.

Material (solution composition)	χ [€/g*]	
	exp.	limit
2 mM YAG	0.989	0.920
2 mM GGAG	2.685	2.497
hydrozincite, Zn ₅ (OH) ₆ (CO ₃) ₂		
10 mM Zn ²⁺ , 0.2 M H ₂ O ₂	3.697	1.663
50 mM Zn ²⁺ , 0.5 M H ₂ O ₂	1.337	1.125
zinc peroxide, ZnO ₂		
20 mM Zn ²⁺ , 1 M H ₂ O ₂	11.52	3.389
50 mM Zn ²⁺ , 1 M H ₂ O ₂	4.805	1.647

* mass of final product (garnet or ZnO)

4) Energy consumption, costs $\varepsilon+\tau$ [kWh_e/g, €/g]

The energy costs of the production ε are inevitably higher than what would the photochemical production yield Y suggest, due to the power consumption of the chiller, stirrer and pumps as well as the low efficiency of the UV lamps ($\leq \sim 30\%$). In the described photochemical pilot plant, the power consumption of the system is $P \sim 3.45$ kW (1230 W for the lamps, 170 W for the stirrer motor, 2000 W for the chiller unit and ~ 50 W for the pump), while the light output at 254 nm is just $P' = 336$ W. The energy cost of the production in the described pilot plant is then $\varepsilon \sim (2.85 / Y)$ according to:

$$\varepsilon [kWh_e/g] = \frac{P}{3.6 \cdot Y [g/MJ_{UV}] \cdot P'}$$

Apart from increasing the efficiency of the photochemical reactions (e.g. a more effective photosensitizer), there is no facile way how to significantly improve this contribution to the process cost.

Proper composition or properties of the product also necessitate thermal treatment / calcination at conditions appropriate to the given material. ZnO₂ has been found to require a very slow and careful heating to 200 °C in order to prevent its ejection from crucibles (highly exothermic decomposition into ZnO), while garnet precursors have to be calcined at ~ 1200 °C to fully transform into garnet phase and possess the required luminescence properties. The energy cost associated with heat treatment τ depends on the furnace type, construction, loading and available volume, heat insulation and also on the temperature program used. While one furnace may be used for thermal treatment of various described materials, its properties cannot be ideal for all these materials. For simplicity, we estimated thermal treatment costs under the following assumptions:

- A. A single furnace type (high-temperature chamber furnace) was selected for all materials.
- B. The properties of Carbolite RHF 14/8 were used as a model furnace for the cost calculations (8000 W max power, 6-litre working chamber, max. 1300 °C in continuous regime).
- C. The power consumption during dwell time at any temperature was estimated from “holding power” of RHF 14/8, 15/8 and 16/8 models by a 2nd degree polynomial fit. Idle power consumption at 25 °C was assumed to be ~ 0.2 kW; thus, the power consumption formula is $P_{\text{est}} = 1.19 \times 10^{-6} T^2 + 4.59 \times 10^{-4} T + 0.2$ kW.
- D. The power consumption during the heating up phase was estimated through a combination of a short period of full-power heating (58 °C / min, $P_{100\%} = 8$ kW) and a short hold at the given temperature (P_{est}) so that the final temperature increase within the cycle time is precisely equal to the desired ramp rate.
- E. The heating ramp rate was chosen as 15 °C / min for all materials except ZnO₂, for which 2 °C / min was used.
- F. The furnace cooldown after the heat treatment is finished was assumed to be non-regulated and its

duration was approximated as $\sim \{\text{max. temperature} / 100 \text{ °C}\}$ hours.

- G. The furnace load was assumed as a ~ 4 cm thick layer of powder in a single large high-walled crucible of 10×24 cm cross-section that fills the useable area of the furnace with a clearance of 1.5 cm on all sides. The packing density of ~ 6% theoretical density of the final product was also assumed, which is an approximate packing density of the synthesized powders.

The thus obtained values of ε , τ (see Table SI6) were then converted into energy cost of production and treatment [€/g] using early 2021’s price of ~ 57 €/MWh on electricity market in Central Europe.

Table SI6 – The energy costs for synthesis of studied nanomaterials along with their theoretical limits for 100 % yield.

Material (solution composition)	ε [kWh/g*]		τ [kWh/g*]	$\varepsilon_{\text{exp}} + \tau$ [€/g*]
	exp.	limit		
2 mM YAG	0.852	0.792	0.033	0.050
2 mM GGAG	0.572	0.532	0.022	0.034
hydrozincite, Zn ₅ (OH) ₆ (CO ₃) ₂				
10 mM Zn ²⁺ , 0.2 M H ₂ O ₂	0.778	0.350	0.012	0.045
50 mM Zn ²⁺ , 0.5 M H ₂ O ₂	0.063	0.053		
zinc peroxide, ZnO ₂				
20 mM Zn ²⁺ , 1 M H ₂ O ₂	1.894	0.557	0.004	0.108
50 mM Zn ²⁺ , 1 M H ₂ O ₂	0.752	0.255		

* mass of final product (garnet or ZnO)

5) Labour costs λ [€/g]

The costs associated with staff operating the pilot plant was evaluated using the following assumptions: one person only is needed for any task at any given time, the hourly labour cost of an industrial worker is 28.2 €/h (Eurostat 2019 average for 28 states) and this cost was multiplied by 51 / (49 - 5) = 1.16 to account for holidays and 5-week vacation. On average, 1 hour is needed for weighing and measuring the chemicals for a given synthesis, 1 hour is required for setting up the pilot plant,

and 1 more hour is needed for draining the irradiated solution into barrels and starting the clean-up. Naturally, this essentially fixed labour cost clearly favours syntheses with a large amount of product produced in one run; therefore, garnets with doubled concentrations were also included in Table SI7 for comparison. We also assumed that overseeing the pilot plant would occupy the operator ~ 5 % of the whole run time.

The product separation from the irradiated solution represents another associated labour cost, because it requires a near-constant oversight in a laboratory-scale operation. The character of the product and requirements of the final customer determine the method needed for product separation; the assumed time (labour costs) requirements are based on our experience with processing of solutions from the described photochemical pilot plant. The first step, partial product sedimentation in the solutions and subsequent decantation, does not require human oversight and was not included in the labour costs. Similarly, drying of the solid phase obtained after product separation is not associated with any labour costs.

In the case of particulate product (ZnO_2 , solid precursors for garnets with high concentrations), classical vacuum filtration with Millipore HAWP filters (0.45 μm) is a sufficient method. For simplicity, we assumed an equal filtration speed for any product composition of ~ 50 g per hour of human oversight.

Whenever the product is gelatinous (solid precursors for garnets with low concentrations), higher pressure gradient becomes necessary for an efficient filtration without clogging of the HAWP filter or any other filter due to a thin layer of gel. Therefore, the Amicon microfiltration unit with a 500 mL inner volume and 9 cm in diameter, which is on the upper end of laboratory-sized devices, was used for this purpose and routinely yielded ~ 5 g of the final product per hour.

A custom-built industrial-scale microfiltration unit at Tesla V.T. Mikroel (5 L volume, 15 cm diameter), on the other hand, was able to obtain ~ 200 g of product per hour in the case of powder-like material and ~ 100 g of gelatinous product per hour, using Millipore HAWP

filters. This improvement resulted mainly from a much larger surface area of the filter.

Table SI7 – The labour costs for synthesis of studied nanomaterials (setting up, pilot plant overview, draining) and for product filtration using laboratory devices. As a comparison, theoretical limits for 100 % yield of synthesis and industrial-scale microfiltration units are included.

Material (solution composition)	$\lambda_{\text{synthesis}}$ [€/g*]		$\lambda_{\text{filtration}}$ [€/g*]	
	exp.	limit	labor.	indust.
2 mM YAG	1.51	1.41	6.54	0.33
2 mM GGAG	1.02	0.95		
4 mM YAG [†]	0.96	0.89	0.65	0.16
4 mM GGAG [†]	0.64	0.60		
hydrozincite, $\text{Zn}_5(\text{OH})_6(\text{CO}_3)_2$				
10 mM Zn^{2+} , 0.2 M H_2O_2	3.72	1.67	0.65	0.16
50 mM Zn^{2+} , 0.5 M H_2O_2 [†]	0.39	0.33		
zinc peroxide, ZnO_2				
20 mM Zn^{2+} , 1 M H_2O_2 [†]	3.46	1.02	0.65	0.16
50 mM Zn^{2+} , 1 M H_2O_2 [†]	1.25	0.42		

* mass of final product (garnet or ZnO); [†] powder-like morphology

UV lamp layout within the photochemical pilot plant

The homogeneity of the irradiation field was thoroughly considered during the design of reactor lid with sockets for UV lamps. Optical photons are attenuated according to Lambert-Beer's law (assuming the absorbance of solution is reasonably low): $I = I_0 \times 10^{-kx}$, where x is the distance from a (point) source of radiation. Therefore, cost-efficient and absolutely homogeneous irradiation of any large volume is virtually impossible. The absorption spectra of typical solutions for garnet synthesis (equivalent to 1 mmol dm^{-3} of garnet) are shown in Ref. 26, where the absorbance at 254 nm is ~ 0.06 for 1 cm optical path length, i.e. $k = A/l = 0.06 \text{ cm}^{-1}$.

The lower the k value, the more homogeneous the irradiation field is. On the other hand, the extent of photochemical reactions decreases with k as well.

The low-pressure mercury discharges were arranged around the reactor axis in a hexagonal pattern so as to have a *relatively* uniform UV light field across the whole cross-section of the reactor. The separation between lamps with their protective quartz tubes ($\varnothing \sim 2.5$ cm) was chosen as ~ 6.7 cm; therefore, the distance between quartz tubes was ca. 4 cm. The design of the reactor is depicted in Fig. SI_1.

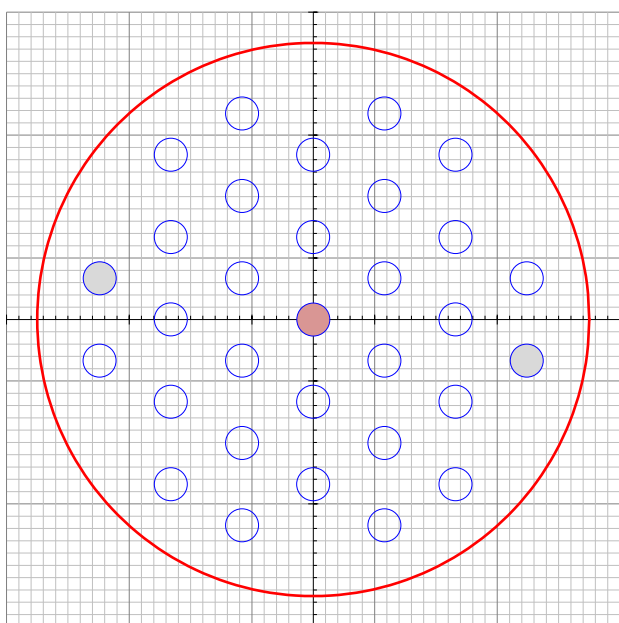


Fig. SI_1 – The horizontal cross-section of the photochemical pilot plant with lamp positions (empty circles), the central stirring shaft (filled red circle) and two inlet valves (filled grey circles).

The UV light intensity within the irradiation field was simulated by a simplistic model that assumes:

- a) Absorption coefficient of solutions $\sim 0.06 \text{ cm}^{-1}$
- b) No scattering or reflection events were considered
- c) Only the first layer of lamps around a particular lamp was considered
- d) The outer-rim lamps were not simulated

The simplified map of relative intensity of UV light (0 – 100 %) around the central shaft is shown in Fig.

SI_2 and in a full configuration of 1+6 UV lamps is shown in Fig. SI_3. The colour bands correspond to 10 % of the intensity, meaning that the simulated irradiation field is reasonably homogeneous within 80 – 100 % (7 lamps). When the [0,0] spot contains no source of radiation (the stirring shaft), the area around it has 75 – 80 % of maximum intensity.

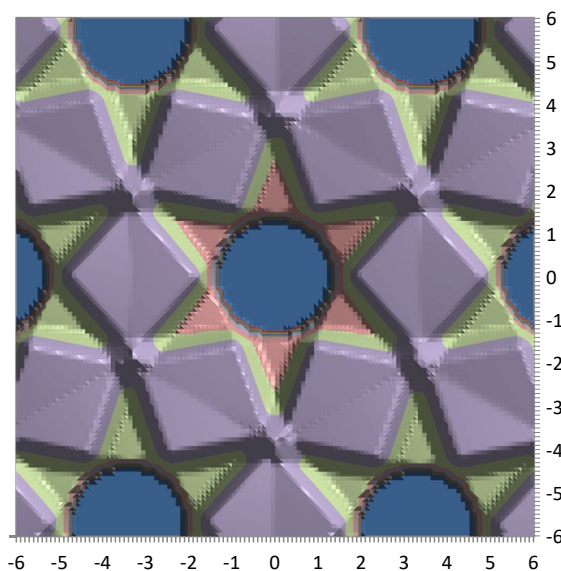


Fig. SI_2 – Simulated distribution of UV light intensity within the photochemical reactor around the stirring shaft (no source of radiation at [0,0]); colour bands represent 10 % intervals.

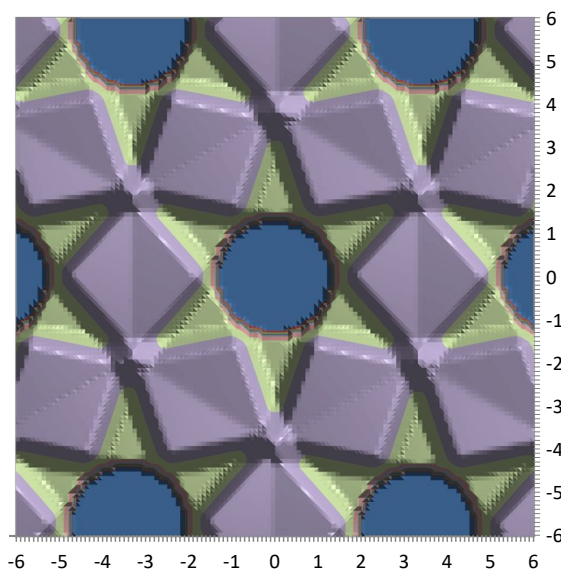


Fig. SI_3 – Simulated distribution of UV light intensity within the photochemical reactor around a UV lamp at [0,0]; colour bands represent 10 % intervals.